

PAPER • OPEN ACCESS

On solutions to a novel non-evolutionary integrable $1 + 1$ PDE

To cite this article: Francesco Giglio *et al* 2023 *J. Phys. A: Math. Theor.* **56** 485205

View the [article online](#) for updates and enhancements.

You may also like

- [Geophysical investigations to study the physical–mechanical characteristics of the rock in a coastal environment: the cliff of Roca \(Lecce, Italy\)](#)
Giovanni Leucci
- [Experimental analysis of a TEM plane transmission line for DNA studies at 900 MHz EM fields](#)
F Belloni, D Doria, A Lorusso et al.
- [The newly installed IBIL \(Ion Beam Induced Luminescence\) set-up at CEDAD-University of Salento: design and first applications on perovskite](#)
G. Quarta, A.P. Caricato, C. Provenzano et al.

On solutions to a novel non-evolutionary integrable $1 + 1$ PDE

Francesco Giglio¹ , Giulio Landolfi^{2,*} 
and Luigi Martina² 

¹ School of Mathematics and Statistics, University of Glasgow, Glasgow, United Kingdom

² Dipartimento di Matematica e Fisica 'Ennio De Giorgi' Università del Salento and I.N.F.N. Sezione di Lecce, via Arnesano I-73100 Lecce, Italy

E-mail: giulio.landolfi@le.infn.it and giulio.landolfi@unisalento.it

Received 1 August 2023; revised 13 October 2023

Accepted for publication 18 October 2023

Published 7 November 2023



CrossMark

Abstract

We investigate real solutions of a C-integrable non-evolutionary partial differential equation in the form of a scalar conservation law where the flux density depends both on the density and on its first derivatives with respect to the local variables. By performing a similarity reduction dictated by one of its local symmetry generators, a nonlinear ordinary differential equation arises that is connected to the Painlevé III equation. Exact solutions are secured and described provided a constraint holds among the coefficients of the original equation. In the most general case, we pinpoint the generation of additional singularities by numerical integration. Then, we discuss the evolution of given initial profiles. Finally, we mention aspects concerning rational solutions with a finite number of poles.

Keywords: diffusive/dissipative $1 + 1$ -PDE models, symmetries of differential equations, similarity solutions, Painlevé equations, poles motion

(Some figures may appear in colour only in the online journal)

* Author to whom any correspondence should be addressed.



Original Content from this work may be used under the terms of the [Creative Commons Attribution 4.0 licence](https://creativecommons.org/licenses/by/4.0/). Any further distribution of this work must maintain attribution to the author(s) and the title of the work, journal citation and DOI.

1. Introduction

We address the study of the nonlinear partial differential equation (PDE)

$$\partial_t v + \partial_x \left\{ \frac{1}{c_1 v + c_3 \sigma} [c_2 v^2 + c_4 \sigma^2 + \sigma \eta (c_1 \partial_t v + c_2 \partial_x v)] \right\} = 0 \tag{1}$$

where $v = v(x, t)$ is a real function of the two real independent variables x and t , and η , σ and the c_j 's are real constants. The equation has been introduced recently in [1] in connection with the problem of describing fluid systems of volume v whose behaviour at pressure $P = x/t$ and temperature $T = 1/t$ deviates from the van der Waals equations of state, the parameter η being there a small positive real parameter identifying the inverse of the number of fluid molecules. Equation (1) extends case studies that are very familiar to researchers in applied mathematics and physics, above all the Bateman–Burgers equation $\partial_t u + u \partial_x u = \eta \partial_{xx} u$ [2–4] whose structure is recovered when $c_1 = 0$. In fact, equation (1) collocates itself naturally within equations that generalise Kolmogorov–Petrovsky–Piskunov reactive–diffusive [5] or nonlinear Fokker–Planck models [6], viz. $\partial_t v + D \partial_{xx} v = f(v)$ and $\partial_t v + D \partial_{xx} v = \partial_x(Fv)$, being D the diffusion coefficient. It is known that these equations find several applications in a number of fields, ranging from condensed matter and liquid crystals physics to population dynamics and social sciences (see e.g. [7–9]), and incorporate various phenomena, such as phase transitions, travelling-wave solutions, shock waves, anomalous diffusion, and so forth.

Owing to the rather general conditions behind its introduction, one can expect that even the PDE (1) may be relevant, or at least of use in the complex systems domain in a wider perspective, not limited to the early motivation in [1]. Indeed, PDE (1) originates merely from two plain requirements:

- (i) the insertion within a scalar conservation law

$$\partial_t v = \partial_x \varepsilon \tag{2}$$

of a simple nonlocal expansion of the flux density

$$\varepsilon = \varepsilon_0(v) + \eta \varepsilon_1(v) \partial_x v + \eta \varepsilon_2(v) \partial_t v + O(\eta^2) + g(t), \tag{3}$$

where ε is assumed be uniquely determined by a function $v = v(x, t)$, depending in its turn on two local variables x and t , and η is a small expansion parameter;

- (ii) the successive singling out of those dynamics that are compatible with the linearisability requirement of the PDE resulting from (2) and (3), via the Cole–Hopf transform

$$v(x, t) = \eta \sigma \partial_x \ln \varphi(x, t), \tag{4}$$

into a linear PDE for the potential function $\varphi(x, t)$, being σ a nonvanishing real parameter.

Remark that, contrary to the models previously mentioned, the C-integrable [10] equation (1) is actually not of evolutionary type, like $\partial_t v = G(x, t, v, \partial_x v, \partial_{xx} v, \dots)$ for which many general results are available in the literature and can be exploited [11–16]. For instance, it is known that a PDE of the form $\partial_t v = \partial_{xx} v + f(v, \partial_x v)$ can be mapped into the *heat* equation or the Bateman–Burgers equations (see, e.g. proposition 4.3 in [11], pp. 170). But from results in [17] regarding the symmetry properties one realises that no local transformations can map (1) into these equations. Notwithstanding, the model can be linearised through the Cole–Hopf transformation (4) with real-valued parameter σ and potential φ , whose actual value and

meaning may be suggested from the specific problem³. As a result of requirements (i) and (ii), function φ fulfils a linear PDE that, interestingly, turns out to be an ‘interpolation’ of the *heat* and *Klein–Gordon* (KG) type equations⁴:

$$\underbrace{\eta c_3 \partial_t \varphi + \eta^2 c_2 \partial_{xx} \varphi}_{\text{heat-type}} + \underbrace{\eta^2 c_1 \partial_{xt} \varphi + c_4 \varphi}_{\text{KG-type}} = 0. \quad (5)$$

Similarly to the Bateman–Burgers case and other C-integrable PDEs, even though there is the possibility to tackle the problem of analysing its solutions by taking great advantage from its linearisability and from a successively nicely posed initial value problem, there are reasons to not overlook the direct study of equation (1). For instance, the dynamical emergence of some peculiar features, such as singularities or shock-type dynamics, may be more perspicuous. Further, the way one can benefit from known results to generate new ones by resorting to symmetry group techniques is affected. The Cole–Hopf transformation is indeed non-local and the spectrum of local symmetry generators of (1) and those of its φ -potential formulation differ, and accordingly the explicit form of the associated invariants. Moreover, similarly to what it has been argued for the Bateman–Burgers equation, issues can be raised in respect to the problem of giving appropriate boundary conditions, due to the nature of the Cole–Hopf transformation [26, 27]. Finally, once the expansion (3) is assumed, but the linearisability requirement for (2) is relaxed, models would outcome whose investigation will advantage of what is already apprehended about (1).

Because of the aforementioned reasons, we are going to look for basic distinguishing attributes exhibited by solution to (1), by paying attention, in particular, to the presence of singularities. To do this, we exploit the knowledge of the symmetries identified in [17], so to perform a suitable reduction leading to a nonlinear ordinary differential equation (ODE). Such an ODE describes the solutions on the orbits of a one-dimensional symmetry subgroup, generated by the simultaneous Galilei and scaling transformation for the x, t, v variables, and it turns out to be connected with the Painlevé III (PIII) equation. In the presence of a certain constraint on the coefficients c_j in (1), solutions can be given in closed form, and their features are discussed. In the most general case, one can proceed by pursuing specific strategies, such as numerical integration or the carrying of a Painlevé test, to understand relevant characteristics, such as the dynamics of poles.

The outline of the paper is as follows. In section 2 we introduce the problem of solving equation (1) by selecting some natural simplifications, driven by conditions on the parameters. In section 3 we focus on solutions pertinent to the orbits of the local symmetry generators resulting for the equation from a symmetry group theoretical approach, by first arguing on what the two simplest generators imply and then deriving the nonlinear ODE describing similarity solutions pertinent the remaining generator. In section 4 we determine the solutions to the obtained nonlinear ODE, once a given condition is satisfied by coefficients c_j , and clarify their features. Implications for the corresponding functions $v(x, t)$ solving equation (1) are in section 5. The most general case is considered in section 6 where, also bearing in mind findings

³ In the real fluid case dealt with in [1], for instance, σ turns out to be connected to the universal gas constant (or equivalently to the Boltzmann thermodynamic constant [17]) while φ plays the role of the statistical partition function.

⁴ The connections between statistical field models and the *heat* or KG equations for the underlying partition function have been pointed out in literature for archetypical complex systems such as the Curie–Weiss model for spins, the van der Waals model for real gases and generalisations, and the Maier–Saupe model and biaxial generalisations for nematic liquid crystals [18–24]. The application of a Cole–Hopf type transform to the 1+1 *heat* and KG equations leads to nonlinear equations in the Burgers hierarchy, that is viscous scalar conservation laws possessing constant viscous central invariant [25].

of section 4, we explore the consequences as regards the properties of the solutions to (1), and their pole and stationary points dynamics. In section 7 we perform remarks concerning the analysis of pole dynamics implied for rational solutions involving multiple poles. In section 8 we summarise the results of our study. Finally, appendix A contains proofs for propositions stated in section 4.

2. Properties of equation (1)—some subclasses of solutions

As we already mentioned, equation (1) represents a generalisation of known diffusive/dissipative models. Several comments can be straightforwardly made in respect to some of its solutions when particular conditions hold on coefficients or when specific dependences on independent variables are sought. Below, we pay attention to the first prospect, the second one being dealt with in section 3.

2.1. Remarks on subcases implied by the vanishing of coefficients c_j

The various real constants present in (1) can assume arbitrary values in general, and depending on the problem to which the model would refer they may acquire particular meaning and major roles under distinct dynamical regimes⁵. By acting on the coefficients c_j , reductions can be performed on equation (1) that significantly affect the differential problem. This immediately eventuates in the following examples.

Example 1: $c_1 = 0$. One ends up into a Bateman–Burgers equation structure, which has originally introduced in [2, 3] and is one among the most investigated canonical integrable nonlinear PDEs. With $c_1 = 0$, equation (1) becomes indeed the nonhomogeneous nonlinear heat equation

$$\partial_t v + \frac{2c_2}{\sigma c_3} v \partial_x v + \eta \frac{c_2}{c_3} \partial_{xx} v = 0 \tag{6}$$

with the thermal diffusion coefficient $-\eta c_2/c_3$. Equation (6) can be converted to a linear diffusion equation by Cole–Hopf transform, as it is widely renowned.

Example 2: $c_2 = c_4 = 0$. Equation (1) becomes

$$\partial_t v + \sigma \eta c_1 \partial_x \left(\frac{1}{c_1 v + c_3 \sigma} \partial_t v \right) = 0. \tag{7}$$

We would like to point out that (7) can be promptly integrated to give

$$v = \sigma \eta \partial_x \ln \left[\beta(x) + \alpha(t) e^{-\frac{c_3}{c_1 \eta} x} \right], \tag{8}$$

being $\alpha(t)$ and $\beta(x)$ arbitrary functions of their variables. It is thence worth to pay attention on the case $c_2 = c_4 = 0$ because, due to the simultaneous presence of two arbitrary functions,

⁵ For example, in the discussion in [1]: (i) setting σ to minus the universal gas constant guarantees that at high temperatures $T = t^{-1}$ and pressures $P = x/t$ an ideal gas behaviour with a core–volume term can be matched with φ being just the associated statistical partition function, and in this regime effects of constants c_j can be neglected; (ii) $c_4/c_1 = a/\sigma^2$, where a denotes the mean-field parameter a entering the van der Waals equation of state $(v - b)(P + av^{-2}) = RT$ for real gases (see also [18]); (iii) sign ansatz on the structural constants c_j are to be considered to guarantee the reaching of critical regime with a real fluid behaviour and to avoid that the partition function so identified in this description diverges.

a number of examples could be given and discussed. We notice, in particular, that simple pole solutions are allowed even on scale other than that induced by the product $\eta\sigma$, as opposite to what results from solutions (18) (even when one among c_2 or c_4 is zero). Precisely, solutions $v = \eta\sigma\gamma/x$ would follow through the choice $\alpha(t) = 0$ and $\beta(x) = x^\gamma$, for some non-zero constant γ .⁶

Example 3: $c_3 = c_4 = 0$. In this case one ends up into a Riccati type equation:

$$\sigma \eta c_1 \partial_\tau v(\tau, t) = f_1(\tau) v(\tau, t) - v(\tau, t)^2, \quad \tau = c_1 x - c_2 t, \tag{9}$$

where f_1 is an arbitrary function of τ . Solutions to (9) can be thus given as

$$v(\tau, t) = c_1 \eta \sigma \partial_\tau \ln \left[f_2(t) + \int^\tau e^{\frac{1}{c_1 \eta \sigma} \int^\tau f_1(x) dx} d\tilde{\tau} \right] \tag{10}$$

being $f_2(t)$ an arbitrary function of variable t .

2.2. The limit $\eta \rightarrow 0$ –weak solutions

For the particular choice $c_1 = 0$, the model equation (1) is nothing but the Bateman–Burgers equation, describing the propagation of nonlinear waves in regime of small viscosity. In the inviscid limit $\eta \rightarrow 0$ weak solutions are thence expected indicating a non trivial complex behaviour for the associated physical system, such as a phase transition [20–22, 28]. A similar picture is expected to hold as well when $c_1 \neq 0$. Indeed, if η is vanishing the implicit solution form

$$v = \tilde{f}[x + c(v)t] \tag{11}$$

is found, where

$$c(v) = \frac{(c_1^2 c_4 + c_2 c_3^2) \sigma^2}{c_1 (c_1 v + c_3 \sigma)^2} - \frac{c_2}{c_1} \tag{12}$$

is a rational characteristic speed and \tilde{f} is an arbitrary function of its argument that is typically provided in the form of initial datum. Remarkably, if the quantity

$$\Delta = c_1^2 c_4 + c_2 c_3^2 \tag{13}$$

vanishes one merely has that the initial datum $\tilde{f}(x)$ propagates at constant speed, i.e. $v = \tilde{f}(x - \frac{c_2}{c_1} t)$. When instead $\Delta \neq 0$ then $\frac{d}{dv} c(v) \neq 0$, and compressive shock or expansive fan solutions are in principle contemplated [29].

3. Similarity reductions

In this section, we would like to pay attention on a special subclass of solutions to equation (1): those that are connected with the reduction of the equation on the orbits of its group symmetry generators. The knowledge of symmetry generators underlying a given differential problem generally proves to be helpful in two complementing respects, indeed. The first possibility is to construct new solutions from known ones [11, 12]. Besides, one can perform a *similarity*

⁶ Among possible noticeable examples, remaining within the original context in which equation (1) was derived, such choice would enable in principle to account for the ideal gas equation of state. However, keeping the values of $\sigma < 0$ and $\eta > 0$ identified in [1], the simple pole term $\eta\sigma/x$ in (18) would have instead wrong negative sign and physical scale.

reduction of the differential problem to find solutions that remain invariant under the action of the symmetry group, known as *similarity solutions*. The identification of such reductions relies on the recognition of the class of invariants $I(x, t, v)$ to a given symmetry generator W , that is such that $WI(x, t, v) = 0$ [12]. Below, we will proceed in this second respect.

Symmetry generators for equation (1) with $c_1c_2c_3c_4 \neq 0$ have been computed in [17]. It turns out that a three-parameter group of symmetry underlies the differential problem (1) through the action of the following three vector fields:

$$W_1 = \partial_x, \quad W_2 = \partial_t + \frac{c_2}{c_1}\partial_x, \quad W_3 = t\partial_t + \left(2\frac{c_2}{c_1}t - x\right)\partial_x + \left(\frac{c_3\sigma}{c_1} + v\right)\partial_v. \quad (14)$$

Each of these operator defines a one-dimensional subgroup $G_k(\{x, t, v\}; \lambda)$ of local transformations depending on a single real parameter λ_k ($k = 1, 2, 3$).⁷

3.1. Similarity reductions from W_1 and W_2

Operators W_1 and W_2 are evidently associated with rigid translations in the x and $t - \frac{c_1}{c_2}x$ directions. The two corresponding invariants $I_1 = I_1(t, v)$ and $I_2 = I_2(c_1x - c_2t, v)$ point to the natural one-dimensional reductions $v = v(t)$ and $v = v(c_1x - c_2t)$. However, both reductions yield to solutions of (1) that are merely constants. Linear combinations of W_1 and W_2 can be considered too. In particular, the operator ∂_t can be obtained, whose invariants imply the reduction $v = v(x)$. The singular behaviour of the resulting similarity solutions can be immediately inferred because equation (1) reduces to the nonlinear ODE of the Riccati type

$$c_2v^2 + c_4\sigma^2 + \eta\sigma c_2\partial_x v = C_0(c_1v + c_3\sigma), \quad (16)$$

where C_0 is a constant. By virtue of this, when $C_0c_2 \neq 0$ solutions $v(x)$ to equation (16) are

$$v(x) = \frac{c_1C_0}{2c_2} - \frac{\tilde{C}_0}{2c_2} \tan \left[\frac{c_1\tilde{C}_0}{2} \left(\frac{x}{c_2\eta\sigma} + C_1 \right) \right], \quad (17)$$

where C_1 is an integration constant and $\tilde{C}_0 = \sqrt{4\sigma c_2(\sigma c_4 - C_0c_3) - C_0^2c_1^2} \neq 0$. If, in contrast, $\tilde{C}_0 = 0$, i.e. if C_0 takes one of the values

$$C_0^{(\pm)} = \frac{2}{c_1^2} \left[-c_2c_3\sigma \pm \sqrt{c_2(c_1^2c_4 + c_2c_3^2)\sigma^2} \right],$$

then one has the simple rational structure

$$v_{\pm} = \frac{c_1C_0^{(\pm)}}{2c_2} + \frac{\eta\sigma}{x - C_1}. \quad (18)$$

The existence of singular real solutions to (1) is thus put in evidence immediately through (17) and (18) for real C_0, C_1, \tilde{C}_0 and C_{\pm} . Analogous results follow from the reductions implied by the invariants associated with other linear combinations of W_1 and W_2 .

⁷ When $\Delta = c_1^2c_4 + c_2c_3^2 = 0$, infinite symmetries come into play: in addition to three generators (14), the family of symmetry generators

$$W^\infty = \left[G_1 + \frac{c_1}{c_2}F_1(t) \right] \frac{\partial}{\partial t} + \left[F_2\left(-\frac{c_1}{c_2}x + t\right) + F_1(t) \right] \frac{\partial}{\partial x} + \frac{c_1}{c_2} \left(v + \sigma \frac{c_3}{c_1} \right) F_2'\left(-\frac{c_1}{c_2}x + t\right) \frac{\partial}{\partial v} \quad (15)$$

is found, being F_1, F_2 arbitrary functions of their argument and G_1 constant.

3.2. Similarity reductions from W_3

The explicit one-parameter group of symmetry transformation implied by the generator W_3 is also straightforwardly inferred,

$$G_3(\{x, t, v\}; \lambda_3) = \left\{ x_{\lambda_3} = e^{-\frac{c_1}{c_2} \lambda_3} x + 2t \frac{c_2}{c_1} \sinh\left(\frac{c_1}{c_2} \lambda_3\right), t_{\lambda_3} = e^{\frac{c_1}{c_2} \lambda_3} t, v_{\lambda_3} = e^{\frac{c_1}{c_2} \lambda_3} v + \frac{c_3 \sigma}{c_1} \left(e^{\frac{c_1}{c_2} \lambda_3} - 1\right) \right\}. \tag{19}$$

But once attention is paid to the similarity solutions for the equation (1) that would result from the generator W_3 , implications are less expeditious. Indeed, the concerned invariants take the form

$$I_3 = I_3 \left[\left(1 + \frac{c_1}{c_3 \sigma} v\right) t^{-1}, \frac{\eta}{c_3} t(c_1 x - c_2 t) \right]. \tag{20}$$

According to (20), and by a convenient normalisation, functions v can be sought of the form

$$v = \frac{\sigma c_3}{c_1} \left[B \frac{\eta c_1^2}{c_3} t \Phi(\xi) - 1 \right], \quad \xi = B t (c_1 x - c_2 t) \tag{21}$$

with B real constant. By doing so, equation (1) turns into the following second order nonlinear ODE for Φ

$$\Phi''(\xi) = \frac{\Phi'(\xi)^2}{\Phi(\xi)} - \left[\Phi(\xi) + \frac{1}{\xi} - \frac{\Delta}{B c_1^4 \eta^2} \frac{1}{\xi \Phi(\xi)} \right] \Phi'(\xi) - \frac{\Phi(\xi)^2}{\xi} \quad \left(' = \frac{d}{d\xi} \right), \tag{22}$$

resembling a PIII equation with all coefficients trivial but one (see e.g. [30–32]). We are thus lead to distinguish two cases on the basis of the values attained by coefficients. Depending on whether or not $\Delta = c_1^2 c_4 + c_2 c_3^2$ vanishes, two distinct differential equations therefore arise:

- equation 1:

$$\underbrace{\Phi''(\xi) = -\frac{\Phi'(\xi)}{\xi} + \frac{\Phi'(\xi)^2}{\Phi(\xi)} - \frac{\Phi(\xi)^2}{\xi}}_{\text{PIII}} - \Phi(\xi) \Phi'(\xi) \tag{23}$$

for $\Delta = 0$ whatever the constant B in (22);

- equation 2:

$$\underbrace{\underbrace{\Phi''(\xi) = -\frac{\Phi'(\xi)}{\xi} + \frac{\Phi'(\xi)^2}{\Phi(\xi)} - \frac{\Phi(\xi)^2}{\xi}}_{\text{PIII}} - \Phi(\xi) \Phi'(\xi) + \frac{\Phi'(\xi)}{\xi \Phi(\xi)}}_{\text{equation (23)}} \tag{24}$$

when $\Delta \neq 0$, upon setting for convenience

$$B = \frac{\Delta}{\eta^2 c_1^4}. \tag{25}$$

In both (23) and (24) the similarity with the PIII equation $P_{\text{III}}(\xi; -1, 0, 0, 0)$ with all but one vanishing coefficients is underlined. It is noteworthy that the constraint $\Delta = 0$ has already

proved to be relevant in the study of (1) as it gives rise to infinite local symmetries connected to the equation [1] (see equation (15) in footnote 7).

In next sections we shall tackle the problem of understanding properties of solutions to (23) and (24), being heedful to the occurrence of singularities.

4. Properties of equation (23) and of its solutions

While equation (23) may appear at first to be uneasy to solve, its solutions prove to possess a simple analytical form that can be straightforwardly determined. The general real solution reads indeed:

$$\Phi_0(\xi; \alpha_1, \alpha_2) = \frac{\alpha_1 - 1}{\alpha_2(\alpha_1 - 1)\xi^{\alpha_1 - \xi}}, \quad \xi = t(c_1x - c_2t) \tag{26}$$

where α_1 and α_2 are real-valued constants of integration and the arbitrary constant B introduced in (21) has been normalised to unity for simplicity. Notice that the two-parameter family of real functions (26) comprises rational functions with simple single poles, namely $\Phi_0 = (\alpha_1 - 1)\xi^{-1}$ or $\Phi_0 = (\xi + \alpha_2)^{-1}$, which can be obtained for $\alpha_2 = 0$ and $\alpha_1 = 0$, respectively. The null solution function arises instead for $\alpha_1 = 1$. It is also worth to point out that a deeper connection between (23) and the PIII equation unfolds through a Cole–Hopf transformation $\Phi(\xi) = [\log(A - W(\xi))]'$ (with A arbitrary constant): the derivative $w(\xi) = W'(\xi)$ of the Cole–Hopf potential function $W(\xi)$ obeys indeed $w'' = (w')^2w^{-1} - w'\xi^{-1}$, the PIII equation with all parameters null.

Before to proceed in shedding light on features of functions (26), the remark is in order that rational non integer values of α_1 make Φ_0 multivalued [33]. Recalling that (26) is the solution to a nonlinear ODE (equation (23)) with prescribed initial conditions that may possibly arise from specific applicative models, we will simply restrict our study to $\xi \in \mathbb{R}$ and $\Phi(\xi) \in \mathbb{R}$, without providing a criterion for selecting specific real roots. In fact, when multi-valuedness occurs, specific representations would be naturally gauged from the motivating application.

Quantitative and qualitative properties of function (26) are discussed separately in the following two subsections.

4.1. Quantitative properties of solution (26)

We proceed by analysing the solution (26) for positive real α_2 and rational α_1 evaluating singularities and stationary points as they vary, starting with the simplest case $\alpha_1 \in \mathbb{Z}$. For simplicity, we will consider the case $\alpha_2 > 0$. A similar scenario, which is not discussed in detail in this work, is expected when $\alpha_2 < 0$. Singularities of solution (26) for integers α_1 are given by the following, accounting for the standard classification of singularities in the complex plane [26, 33].

Proposition 1 (singularities of solution (26) for integer values of α_1). *Let $\alpha_1 \in \mathbb{Z}$, $\alpha_2 > 0$, $\xi^{(0)} = 0$ and $\xi_{\pm} = \pm|(1 - \alpha_1)\alpha_2|^{\frac{1}{1-\alpha_1}}$. The real singularities of the function (26) are listed below.*

- (i) *No singularities on the real line for odd negative integer α_1 .*
- (ii) *One single singularity (pole) for α_1 even negative integer located at $\xi = \xi_-$.*
- (iii) *Two real singularities when α_1 is even positive integer. These are located at $\xi = \xi^{(0)}$ (pole) and $\xi = \xi_+$ (branch point).*
- (iv) *Three singularities on the real line for odd positive integers α_1 . One is located at $\xi = \xi^{(0)}$ (pole) and the other two at $\xi = \xi_{\pm}$ (branch points).*

Proof. Singularities of (26) for negative integer values of α_1 are identified by real roots of the polynomial $\mathcal{P}^-(\xi) := \xi^{1-\alpha_1} - \alpha_2(\alpha_1 - 1)$, which has complex roots $\xi_l = |(1 - \alpha_1)\alpha_2|^{\frac{1}{1-\alpha_1}} e^{i\frac{\pi+2l\pi}{1-\alpha_1}}$, $l = 0, 1, \dots, -\alpha_1$. If α_1 is odd, there are no real roots⁸, hence proving (i). If α_1 is even instead, a real solution is obtained when $\pi + 2l\pi = (1 - \alpha_1)\pi$, that is for $l = -\frac{\alpha_1}{2}$, giving $\xi_- = -|\alpha_2(1 - \alpha_1)|^{\frac{1}{1-\alpha_1}}$. This proves case (ii).

Similarly to cases (i) and (ii), real poles of (26) for positive integer values of α_1 are given by real roots of the polynomial $\mathcal{P}^+(\xi) := \xi [((\alpha_1 - 1)\alpha_2)\xi^{\alpha_1-1} - 1]$. Excluding the trivial case $\alpha_1 = 1$, which corresponds to the null solution $\Phi_0(\xi) = 0$, the root $\xi^{(0)} = 0$ is readily identified for all values of α_1 . The other complex roots of $\mathcal{P}^+(\xi)$ are $\xi_l = |(1 - \alpha_1)\alpha_2|^{\frac{1}{1-\alpha_1}} e^{i\frac{2l\pi}{1-\alpha_1}}$, $l = 0, 1, \dots, \alpha_1 - 2$. A real root is promptly obtained for $l = 0$, that is $\xi_+ = |(1 - \alpha_1)\alpha_2|^{\frac{1}{1-\alpha_1}}$. Another solution for odd α_1 is found requiring $2l\pi = (1 - \alpha_1)\pi$. Such solution reads $\xi_- = -|(1 - \alpha_1)\alpha_2|^{\frac{1}{1-\alpha_1}}$, hence completing the proof of (iii) and (iv). \square

Singularities ξ_{\pm} are clearly *movable* in that they are not fixed by the equation (23), but rather they are determined by the initial condition assigned for the equation itself. In fact, the only *essential* singularity, when present, is at $\xi^{(0)} = 0$, as one can see from (23).

Properties of solution (26) can be further characterised by looking at its stationary points. The stationary points of solution (26) for integer α_1 are provided by the following:

Proposition 2 (stationary points of solution (26) for integer values of α_1). *Let $\alpha_1 \in \mathbb{Z}$, $\alpha_2 > 0$, $\xi^{(0)} = 0$ and $\xi_{\pm}^c = \pm|\alpha_1(1 - \alpha_1)\alpha_2|^{\frac{1}{1-\alpha_1}}$. The stationary points of solution (26) are listed below.*

- (i) *Three stationary points located at $\xi = \xi^{(0)}$ (inflection point) and $\xi = \xi_{\pm}^c$ for α_1 odd negative integer with $\alpha_1 < -1$.*
- (ii) *Two stationary points when $\alpha_1 = -1$, located at $\xi = \xi_{\pm}^c$.*
- (iii) *Two stationary points for α_1 even negative integer, located at $\xi = \xi^{(0)}$ and $\xi = \xi_{\pm}^c$.*
- (iv) *One single stationary point located at $\xi = \xi_{\pm}^c$ for α_1 even positive integer.*
- (v) *Two stationary points for odd positive integers α_1 located at $\xi = \xi_{\pm}^c$.*

Singularities and stationary points of (26) for rational values of α_1 can be also derived as shown in the below:

Proposition 3 (singularities of (26) for rational values of α_1). *Let $\alpha_1 = \frac{q}{p}$ with $q, p \in \mathbb{Z}$ and $\gcd(q, p) = 1$, and consider $\xi^{(0)}$, ξ_{\pm} defined as in proposition 1. The real poles of (26) are listed below.*

- (i) *Case $\alpha_1 < 0$.*
 - (a) *One singularity located at $\xi = \xi_-$ (branch point) if p is odd and q is even.*
 - (b) *No singularities if p and q are odd.*
 - (c) *No singularities if p is even⁹.*

⁸ An equivalent way to see this consists in observing that $\alpha_2(\alpha_1 - 1) < 0$. If $\xi \in \mathbb{R}$ and α_1 is odd, then $1 - \alpha_1$ is even and $\underbrace{\xi^{1-\alpha_1}}_{>0} = \underbrace{\alpha_2(\alpha_1 - 1)}_{<0}$ is inconsistent.

⁹ As we have already pointed out, in this work we are standardly considering for $\xi \geq 0$ and p even, $\xi^{1/p} = \sqrt[p]{\xi}$. If $\xi^{1/p} = -\sqrt[p]{\xi}$ is adopted instead, a second singularity arises at $\xi = \xi_+$.

- (ii) Case $0 < \alpha_1 < 1$.
 - (a) Two singularities if p is odd and q is even located at $\xi = \xi^{(0)}$ (branch point) and $\xi = \xi_-$ (branch point).
 - (b) One singularity located at $\xi = \xi^{(0)}$ (branch point) if p and q are odd.
 - (c) One singularity located at $\xi = \xi^{(0)}$ (branch point) if p is even¹⁰.
- (iii) Case $\alpha_1 > 1$.
 - (a) Two singularities if p is odd and q is even located at $\xi = \xi^{(0)}$ (pole) and $\xi = \xi_+$ (branch point).
 - (b) Three singularities if p and q are odd located at $\xi = \xi^{(0)}$ (pole) and $\xi = \xi_{\pm}$ (branch points).
 - (c) Two singularities at $\xi = \xi^{(0)}$ (pole) and $\xi = \xi_+$ if p (branch point) is even.

Proposition 4 (stationary points of (26) for rational values of α_1). Let $\alpha_1 = \frac{q}{p}$ with $q, p \in \mathbb{Z}$ and $\gcd(q, p) = 1$, and consider $\xi^{(0)}, \xi_{\pm}^c$ defined as in proposition 2. The stationary points of (26) are listed below.

- (i) Case $\alpha_1 < 0$.
 - (a) Two stationary points located at $\xi = \xi^{(0)}$ and $\xi = \xi_+^c$ if p is odd and q is even.
 - (b) Three stationary points located at $\xi = \xi^{(0)}$ (inflection point) and $\xi = \xi_{\pm}^c$ if p and q are odd.
 - (c) Two stationary points located at $\xi = \xi^{(0)}$ and $\xi = \xi_+^c$ if p is even.
- (ii) Case $0 < \alpha_1 < 1$.
 - (a) One stationary point at $\xi = \xi_-^c$ if p is odd and q is even.
 - (b) No stationary points if p and q are odd.
 - (c) No stationary points if p is even¹¹.
- (iii) Case $\alpha_1 > 1$.
 - (a) One stationary point located at $\xi = \xi_+^c$ if p is odd and q is even.
 - (b) Two stationary points located at $\xi = \xi_{\pm}^c$ if p and q are odd.
 - (c) One stationary point at $\xi = \xi_+^c$ if p is even.

Proofs of propositions 2–4 can be given, *mutatis mutandis*, in a similar fashion of proposition 1 and are reported in appendix. Notice that statements in proposition 1 for integer values of α_1 can be also deduced from proposition 3. For instance, case (iii) in proposition 1, i.e. α_1 even positive integer, can be obtained from case (iii.a) requiring p odd (precisely $p = 1$) and q even.

Depending on the values of constants α_1 and α_2 , distinct features are thus displayed for function (26). Some symmetry properties are promptly perceived: an intertwining creates between the problems of revealing asymptotes and stationary points, and mirror situations are designed through sign changes. In particular, remark that one may write

$$\Phi_0'(\xi; \alpha_1, \alpha_2) = -\frac{\Phi_0^2(\xi; \alpha_1, \alpha_2)}{\xi \Phi_0(\xi; \alpha_1, \alpha_1 \alpha_2)}. \tag{27}$$

¹⁰ If $\xi^{1/p} = -\sqrt[p]{\xi}$ is adopted, a second singularity arises at $\xi = \xi_+$.

¹¹ If one considers $\xi^p = -\sqrt[p]{\xi}$ a stationary point is located at $\xi = \xi_+^c$.

4.2. Qualitative properties of solutions (26)

In this subsection we provide a more circumstantial picture of solutions (26) by complementing with figures previous results concerning the individuation of their singularities and stationary points.

In figure 1 it is shown what is implied for the function Φ_0 of equation (26) whenever $\alpha_2 > 0$ (which, for simplicity, has been set there to the unit value without loss generality). Plots there reveal up to three vertical asymptotes, and the possibility to develop local maxima and minima, as reckoned in the previous section 4.1. First five plots refer to the case where α_1 is an integer number, for which propositions 1 and 2 hold. Figure 1(a) displays the continuous curves generated for negative odd integers α_1 , and the amplification is marked as long as α_1 takes lower and lower values. The effect magnifies itself about the local maximum and minimum points, located at $\xi_{\pm}^c = \pm|\alpha_1(1 - \alpha_1)\alpha_2|^{\frac{1}{1-\alpha_1}}$, showing the transition from smoother curves to shapes with sharp peaks. The changes call for a net bending towards the ξ -axis of wider portion of curves about the origin before to reach the stationary points at faster rate. The null asymptotic values $\Phi_0(\xi \rightarrow 0; \alpha_1, \alpha_2) = 0$ are approached close later of course. Curves turn out to be symmetric under the combined action of reflections of the dependent and independent variables, $\xi \rightarrow -\xi$ and $\Phi_0 \rightarrow -\Phi_0$. Figure 1(b) indicates instead what happens for negative even integers. Comparison is made with the rational function with single pole in $\xi_0 = -\alpha_2$ obtained for $\alpha_1 = 0$. While the right portion of profiles share the features discussed for the prior case, something different happens in the negative ξ -domain, where a vertical asymptote generates and no minimum forms. Decreasing ξ from the origin, the function Φ_0 does no longer decrease but is lifted up, with a final boost on its rate while getting sufficiently close to the vertical asymptote. Passing to the positive odd integer α_1 , see figure 1(c), we go back to a picture where Φ_0 is an odd function of its argument ξ . Both a maximum and a minimum are comprised, but the curve splits into four portions owing to the appearance of three vertical asymptotes, at the origin and at points $\xi_{\pm} = \pm|(1 - \alpha_1)\alpha_2|^{\frac{1}{1-\alpha_1}}$. Two vertical asymptotes are rather concerned for positive even integers α_1 , at the origin and at ξ_{+}^c , a negative maximum laying down in between, see figure 1(d). Moreover, while moving to higher values of α_1 , a step progressively forms about $\xi = -1$, as visible in figure 1(e) and consistently with (26).

The remaining three plots, figures 1(f)–(h), deal with the case $\alpha_1 \in \mathbb{Q}$, thus relying on propositions 3 and 4 in section 4.1. To proceed, we assign to each $\alpha_1 \in \mathbb{Q}$ a unique pair of integers q, p such that $\alpha_1 = q/p$, with $p > 0$ and $\text{gcd}(q, p) = 1$. When q and p are both odd the analogy is with the case of odd integers α_1 . Precisely, if q is odd positive (see black curve in figure 1(f)) then the behaviour resembles the one of of figure 1(c) for odd integers $\alpha_1 > 1$. In a similar way, when q is an odd negative (red curve in figure 1(f)) the likeness is with 1(a) treating odd negative integers α_1 ¹². Correspondingly, when p is odd and q is even, the behaviour of even integers α_1 is recovered. For instance, when $\alpha_1 < 0$ the curves originating for $\Phi_0(\xi; \alpha_1, 1)$ (red curve in figure 1(g)) are alike those for negative even α_1 in figure 1(b). On the contrary, for positive $\alpha_1 < 0$ (black curve in 1(g)) the resemblance is with shapes arising for even positive α_1 (figure 1(d)). Outcomes when $0 < \alpha_1 < 1$ have to be commented separately. Blue curves in figures 1(f)–(h) show the singularity at the origin $\xi^{(0)} = 0$, and possibly a second one at ξ_{-}^c if p and q are odd and even, respectively. In the latter occurrence, the singularity at ξ_{-} remains visible for small values of α_1 , in that $\xi_{-} = -|(\alpha_1 - 1)\alpha_2|^{\frac{1}{1-\alpha_1}} \simeq -|\alpha_2|$. In contrast, $\xi_{-} \rightarrow 0^{-}$ when α_1 approaches the unity from below.

¹² The cases $p = 1$ should indeed reproduce what is known for integers α_1 .

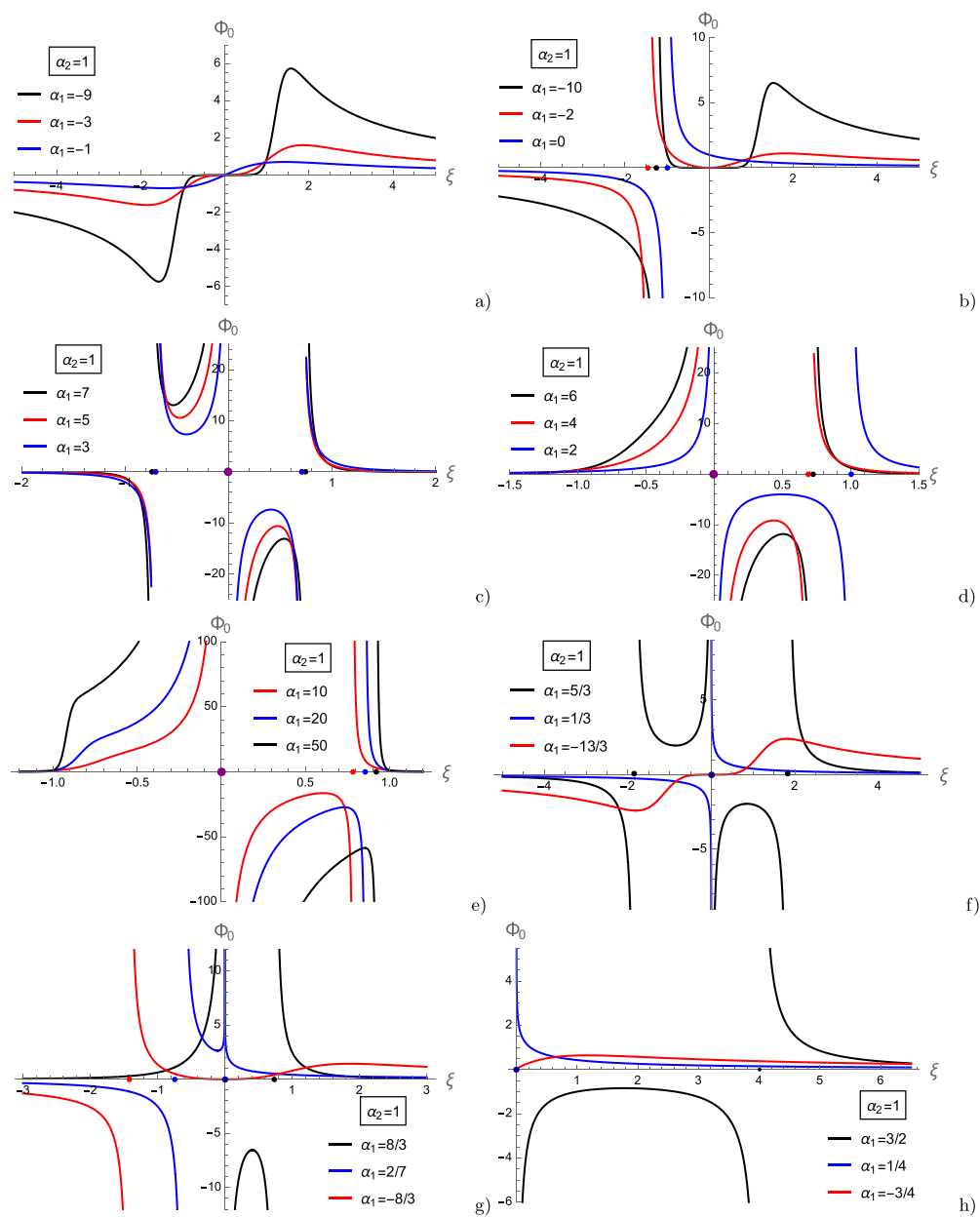


Figure 1. Plots of function $\Phi_0(\xi)$ of equation (26) for $\alpha_2 = 1$. Coloured dots refer to the asymptotes location evinced through propositions 1 and 3 given in section 4.1. (a) α_1 negative odd integer; (b) α_1 negative even integer; (c) α_1 positive odd integer; (d) α_1 positive even integer; (e) birth of a step for higher values of α_1 positive even integer; (f)–(h) rational values $\alpha_1 = q/p$ with q and p integers s.t. $\gcd(q, p) = 1$: (f) q and p both odd; (g) p odd and q even; (h) p even and q odd.

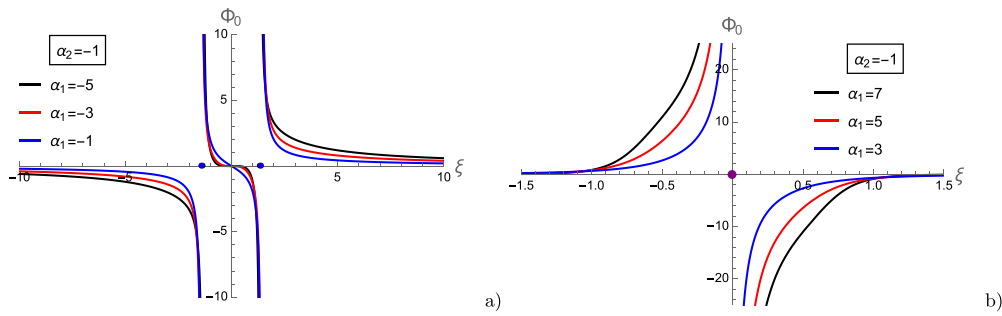


Figure 2. Plots of function $\Phi_0(\xi)$ of equation (26) for $\alpha_2 = -1$. Coloured dots refer to the asymptotes location. (a) α_1 negative odd integer; (b) α_1 positive odd integer.

The scenario arising for functions $\Phi_0(\xi)$ given by equation (26) with negative values of α_2 can be understood from figure 2. We proceed concisely on the grounds of symmetries and analytical information gained for $\alpha_2 > 0$. We start with by remarking indeed that for $\alpha_2 < 0$ and integers j

$$\Phi_0(\xi; 2j, \alpha_2) = -\Phi_0(\xi; 2j, -|\alpha_2|). \tag{28}$$

Therefore, curves for Φ_0 when $\alpha_2 < 0$ and α_1 are even integers result from plots (b) and (d) of figure 1 upon performing joint reflections $\xi \rightarrow -\xi$ and $\Phi_0 \rightarrow -\Phi_0$. As for negative odd integers α_1 , the two vertical asymptotes in figure 2(a) are placed at ξ_{\pm} . Opposite to figure 1(d) which also furnished us two-asymptote depiction for the function Φ_0 , there is no trait designing a stationary point. Finally for the case $\alpha_2 < 0$, one asymptote and two monotonically growing curves are typified by positive even integer values of α_1 , figure 2(b).

5. Solutions (21) to equation (1) when $\Delta = 0$

The clarification of the behaviour allowed for $\Phi_0(\xi)$ put the basis for the understanding of solutions $v(x, t)$ to equation (1) that are or the form (21) and pertinent to the case $\Delta = c_1^2 c_4 + c_2 c_3^2 = 0$. While conveying particulars of $\Phi_0(\xi; \alpha_1, \alpha_2)$ to solutions of (1) via (21), values and signs of constants c_j clearly matter. The role of the evolutionary variable t is also evident in altering the magnitude and moving the poles of resulting solutions $v(x, t)$. As a matter of fact, the changeover from the similarity coordinate ξ to the original independent variables x and t implies that to every point in the ξ -axis it is associated a curve $x(t)$ in the (t, x) plane (at $t \neq 0$): the straight line $c_1 x = c_2 t$ for the point $\xi = 0$, and the composition of the same translational motion with an hyperbolic curve for any other point ξ . Hence

$$x(t) = \frac{1}{c_1} \left(c_2 t + \frac{\xi}{Bt} \right) \tag{29}$$

- (i) when ξ/Bc_1 and c_2/c_1 are both strictly positive, then $x(t)$ is strictly positive (negative) over all the positive (negative) t -domain;
- (ii) if $\xi/Bc_1 > 0$ and $c_2/c_1 < 0$, then $x(t) > 0$ when either $t < -\sqrt{-\xi/Bc_2}$ or $0 < t < \sqrt{-\xi/Bc_2}$;
- (iii) if $\xi/Bc_1 < 0$ and $c_2/c_1 > 0$, then $x(t) > 0$ when either $-\sqrt{-\xi/Bc_2} < t < 0$ or $t > \sqrt{-\xi/Bc_2}$;

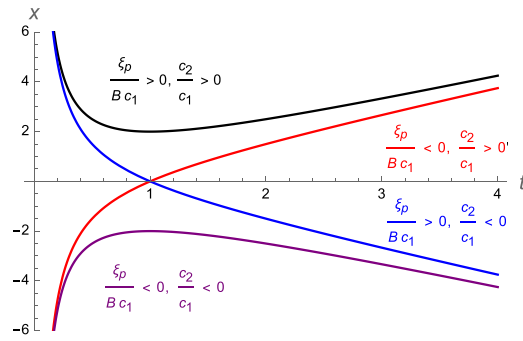


Figure 3. Qualitative motion for $t > 0$ of a point ξ_p on the ξ -axis as it is implied by equation (29). Case (i) (black): $\xi_p/Bc_1 > 0$ and $c_2/c_1 > 0$; case (ii) (blue): $\xi_p/Bc_1 > 0$ and $c_2/c_1 < 0$; case (iii) (red): $\xi_p/Bc_1 < 0$ and $c_2/c_1 > 0$; case (iv) (purple): $\xi_p/Bc_1 < 0$ and $c_2/c_1 < 0$.

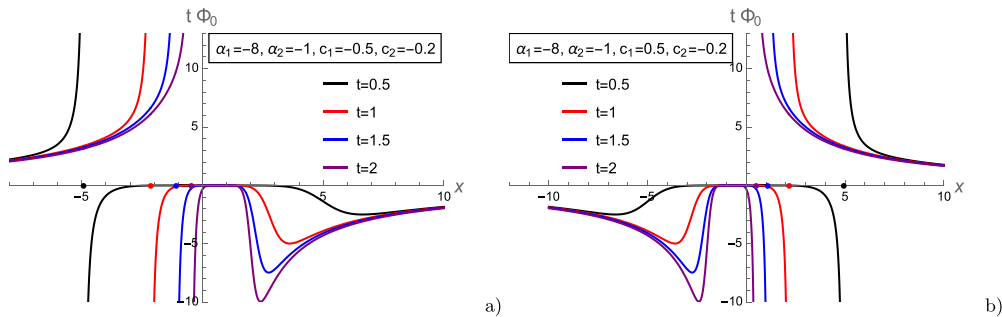


Figure 4. Examples of graphs of function $t\Phi(x, t)$ that follows from (26) at different times and for different choices of parameters c_1 and c_2 . Equation (26) has been taken with $\alpha_1 = -8$ and $\alpha_2 = 1$, for which the shape of $\Phi(\xi)$ is analogous to curves of figure 1(b). Coloured dots refer to the asymptotes location. (a) Progressive deformation of shape for $t\Phi(x, t)$ when c_1 and c_2 are both negative. (b) Progressive deformation of shape for $t\Phi(x, t)$ when $c_1 > 0$ and $c_2 < 0$.

- (iv) if ξ/c_1 and c_2/c_1 are both strictly negative, then x_s is strictly negative (positive) over all the positive (negative) t -domain;
- (v) if $\xi = 0$, then $\text{sign}(x(t)) = \text{sign}(c_1 c_2 t)$.

Qualitative behaviour of $x(t)$ concerned with $\xi \neq 0$ is summarised in figure 3. In particular, the above schematics apply to connote the relocation on the x -axis of singularities of similarity solution (21) while t varies. We thus see that in cases (i) and (iv) the same value of x can be obtained for two distinct values of the local variable $t > 0$, meaning that a reversal of the singularity motion is exhibited. In cases (ii) and (iii), instead, there is a one-to-one correspondence based on a monotonic behaviour for the function $x(t)$ of equation (29).

We are now in the position to outline more efficiently the significant aspects of similarity solution (21) when $\Delta = 0$. Regardless obvious remarks in respect of consequences due to signs of the constants c_j , it is helpful to consider an example of just the function $t\Phi_0 = t\Phi_0(x, t)$. In figure 4, a case based on curves Φ of the type figure 1(b) is considered, in particular by setting $\alpha_1 = -8$ and $\alpha_2 = 1$. Plots there supply a glimpse into effects of sign changes for the

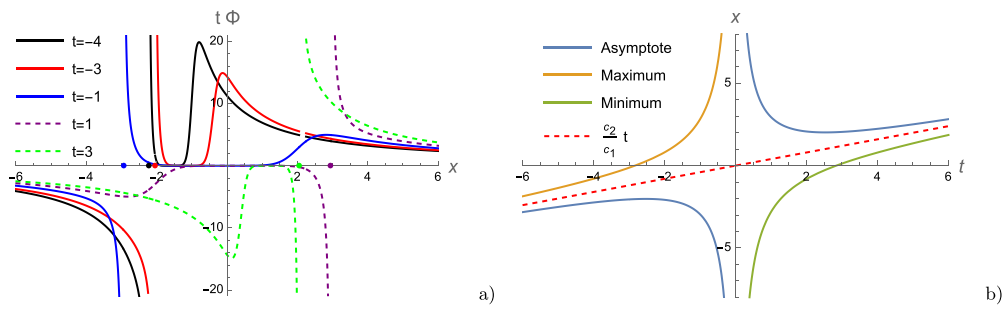


Figure 5. Asymptotes and stationary points motion for the function $t\Phi(x, t)$ arising from (26) with $\alpha_1 = -8, \alpha_2 = 1, c_1 = 0.5$ and $c_2 = 0.2$. (a) The function $t\Phi_0$ for different values of t . For increasing negative t the maximum flattens and shifts the location to higher values of the coordinate x . The asymptote moves as well, but after moving to the right on the x -axis (see the red curve determined at $t = -3$ on the right of the black one obtained for $t = -4$) it reverses its motion and directs itself to the opposite direction (see the blue curve at $t = -1$ on the left of the previously mentioned black and red ones). (b) Motion in the (t, x) plane of asymptote and stationary points, signalling the inversion of motion only for the former.

constants $c_{1,2}$ at positive t . For completeness, and being more instructive, the spectrum of the real ‘evolutionary’ variable t shall be permitted to comprise negative values. To this, we will consider coefficients c_1 and c_2 be both positive, as shown in figure 5. In the formal limit $t \rightarrow -\infty$, resulting function $t\Phi_0(x, t)$ is null. For negative but increasing t ’s, profiles like curves in figure 1(b) tend to form, with lower and lower values attained by the maximum which moves to the right becoming smoother. The generated asymptote first moves to the right either, then reverses its motion by progressively placing itself at lower and lower values of x . At $t = 0$, the asymptote and the maximum (experiencing the ongoing magnitude suppression) are pushed at infinity, and the function lies again on the x axis. At later t , curves are no longer similar to those of figure 1(b), but rather to those ones one gets from them through the simultaneous reflections about horizontal and vertical axes. An asymptote is brought back in the picture from ∞ , approaching a stationary point which is reinstated, but as a minimum moving from $-\infty$ towards the direction of the increasing x becoming narrower and narrower. The asymptote again experiences a ‘bouncing back’ mechanism and an inversion of its motion, but without starting to departing from the minimum (see figure 5). In the formal asymptotic limit $t \rightarrow \infty$, the curve again flattens down on the abscissa. Analogous analysis can be worked out by choosing other pairs of parameters α_1 and α_2 .

6. Properties of equation (24) and its solutions

Evidently, equation (24) is a non-trivial nonlinear ODE. Contrary to equation (24), we have not found a transformation connecting it to the list of Painlevé equations. Of course approximate methods can be resorted in the attempt to have a glimpse of possible dynamics emerging from it. For instance, Painlevé-like test arguments (see e.g. [34, 35] and references therein for an account on this subject) can be carried out while aimed at highlighting features of its solutions, such as their singularity structure. *A priori* equation (24) can have solutions with movable singularities which vary with the initial conditions. Testing the singularity structure of the equation appears particularly meaningful, as it is natural to wonder about admissible deviations

and generalisations with respect to the very basic case (18) displayed, for the one-dimensional reduction of the problem discussed in section 3.1. Having this in mind, the formal expansion

$$\Phi(\xi) = (\xi - \xi_0)^{-j} \sum_{k=k_0}^{\infty} f_k (\xi - \xi_0)^k, \tag{30}$$

being the f_k 's constants, can be thence resorted to identify all possible dominant balances, i.e. the singularities whose form behaves like $\Phi \propto (\xi - \xi_0)^{-j}$. It is readily seen that demanding j to be a positive integer leads to the identification $j = 1$, so that the singular dominant behaviour is associated with a single pole. Going further in the analysis, the *resonance* $r = 1$ is found (in addition to $r = -1$). So, the two arbitrary constants entering the Laurent series representation of the solution (30) with $j = 1$ are given by the movable pole ξ_0 and the coefficient f_1 . To our aims, it is significant to focus on the role of dominant term about a singular point ξ_0 in the local representations of Φ ,

$$\Phi(\xi) \cong \frac{1}{\xi - \xi_0}. \tag{31}$$

That is, for (21) and assuming $\Delta \neq 0$, we can take for equation (1) the approximate solution

$$v(x, t) \cong \frac{\eta\sigma c_1 t}{t(c_1 x - c_2 t) - \xi_0^*} = \frac{\eta\sigma}{x - x_s(t)} \tag{32}$$

about a singular point (the term $\sigma c_3/c_1$ can be patently omitted), being $\xi_0^* = \eta^2 c_1^3 \Delta^{-1} \xi_0$ and $x_s(t)$ given by formula (29) with $\xi/B \rightarrow \xi_0^*$, i.e.

$$x_s(t) = \frac{1}{c_1} \left(c_2 t + \frac{\xi_0^*}{t} \right) \tag{33}$$

($c_1 \neq 0$). At any given $t \neq 0$, the singularity shows up when the real variable x attains the finite value $x_s(t)$. When $\xi_0^* = 0$, the pole $x_s(t)$ simply depends linearly on t and translates with constant velocity c_2/c_1 . If $\xi_0^* \neq 0$ the quantity x_s can be positive or negative depending on the signs of ξ_0^*/c_1 and c_2/c_1 . The motion of poles of the rational solution (32) is easily inferred. We thus see that when ξ_0^*/c_1 and c_2/c_1 are either both positive or both negative (cases (i) and (iv) of previous section) the same value of x_s can be obtained for two distinct values of the local variable $t > 0$, meaning that a reversal of the pole motion is exhibited. When $\xi_0^*/c_1 > 0$ and $c_2/c_1 < 0$ or $\xi_0^*/c_1 < 0$ and $c_2/c_1 > 0$ —cases (ii) and (iii)—there is instead a one-to-one correspondence based on a monotonic behaviour for the function $x_s(t)$. Qualitative behaviour of $x_s(t)$ when $t > 0$ and $\xi_0^* \neq 0$ is as in figure 3. Also remark that when $\Delta = c_1^2 c_4 + c_2 c_3^2 = 0$ the coefficients c_3 and c_4 play no role on the identification and on the motion of the pole $x_s(t)$ as they do not enter in the definition of neither the variable, which now reads $\xi = t(c_1 x - c_2 t)$, nor in defining a normalised value ξ_0^* of the pole ξ_0 (since now one would have (29) with $\xi \rightarrow \xi_0$).

To gain a picture of how its solutions evolve away from a singularity of the type (31), a numerical integration of equation (22) can be performed. Remark that equation (22) does not admit invariance neither under reflections $\xi \rightarrow -\xi$ nor under translations $\xi \rightarrow \xi + \delta\xi$.

Figure 6 pertains solutions Φ to equation (24) obtained with initial condition of the simple pole type about $\xi_0 < 0$. That is, initial conditions have been imposed by assigning that, at a point very close to a certain $\xi_0 > 0$, solutions Φ and Φ' assume the same values of the function $(\xi - \xi_0)^{-1}$ and of its differential. The initial condition matching takes place very close to singularities and for solutions values rather above the domain considered in plots. Integration is performed by increasing the variable ξ from a pole until a successive singularity develops. Numerical integration of (24) in the positive and negative domains of the variable ξ are

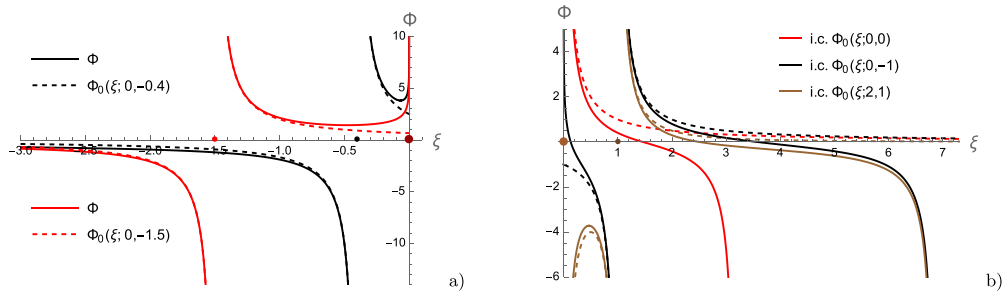


Figure 6. Numerical integration of equation (22) upon superimposition of initial conditions based on functions (26) for distinguished choices of parameters. Functions used to set initial conditions are represented by the dashed curves. (a) Negative simple poles in $\xi_0 = -0.4$ (black) and $\xi_0 = -1.5$ (red). (b) Comparison of curves obtained by superimposing initial conditions either matching simple pole functions at $\xi_0 = 0, 1$ (red and black curves, respectively) or (26) with $\alpha_1 = 2$ and $\alpha_2 = 1$ (brown) which possess both those singularities.

performed separately. In particular, figure 6(a) refers to the case $\xi_0 < 0$. To the left of this singularity, solutions essentially comply with the simple pole function $(\xi - \xi_0)^{-1}$. The plot also tells how the solution runs to a novel singularity located at the origin. When ξ increases and begins to be distant enough from $\xi_0 < 0$ the memory of the pole begins to get lost, and a change of convexity anticipates a growth at a noticeably high rate while approaching the singular point $\xi = 0$. Red and black curves in figure 6(b) report results one obtains by integrating equation (24) over the domain $\xi > 0$ after superimposing initial conditions of the simple pole type $\Phi \simeq (\xi - \xi_0)^{-1}$, with $\xi_0 > 0$. After increasing ξ a while, the portion of solutions that develops to the right of the point $\xi_0 > 0$ are pushed down and directed to a singular behaviour, with a character resembling to tan-type functions. A translation of the singular point ξ_0 provokes a dilation of the interval between the initial and the newly formed singularities (see the red and black curves in curves in 6(b)). Confronted with (23) with the same initial conditions, it can be thus concluded that there is a substantial role played by the last term in equation (24) that sustains the generation of an additional singularity at the origin $\xi = 0$.

6.1. Sensitivity to initial conditions

Discussing solutions to equation (24) would clearly benefit of taking into account initial conditions other than those used so far. At the beginning of this section, we have seen that simple pole behaviour can be extracted for solutions to equation (24). But we have also learned in section 4 how singularities of different types originate for functions Φ when $\Delta = 0$. It makes therefore sense to look at solutions to equation (24) based on sampling of initial conditions establishing a more direct connection with general solutions to the problem (23). For instance, we set initial conditions for (24) demanding solution values and their first derivatives as given by the function (26) near a singularity. After doing so, families of numerical solutions to equation (24) follow that can be seen as deformations of the solutions (26), from which they are expected to inherit some major features. Figure 6(b) considers also what is obtained by this strategy. While not a substantial dependence on this new initial condition, compared to the simple pole initial condition, is displayed to the right of the singularity (see the brown and black tan-type shapes on the right of figure 6(b)), quite a difference is manifested on its left side. As solid and dotted brown curves in figure 6(b) show for smaller ξ , solutions to (24) associated with

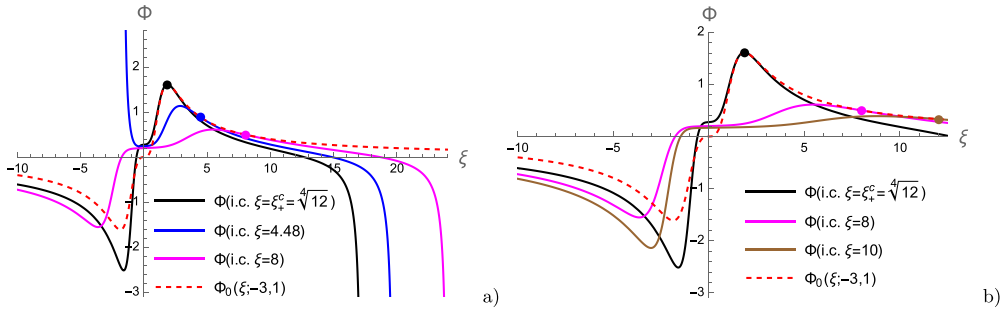


Figure 7. Comparison between functions solving (24) and solution (26) pertinent to $\Delta = 0$. $\Phi(\xi)$ and $\Phi_0(\xi; -3, 1)$ are required to pass both through chosen individual points (coloured disks) with the same rate. The black curve denotes the solution demanded to possess the same maximum (black disk) of $\Phi_0(\xi; -3, 1)$ (red dashed) at $\xi = \xi_+^c = 12^{1/4}$. (a) Deformation of the reference profile $\Phi_0(\xi; -3, 1)$ and sudden appearance of a dissimilar curve (blue). (b) Dynamics of the minimum by varying initial conditions. Lowering the maximum does not necessarily introduce an overall smoothing of Φ in the $\xi < 0$ domain (compare magenta and brown curves).

initial data as given by Φ_0 tend to stay adherent to Φ_0 itself, thence preserving their same singular behaviour approaching the origin. A striking dissimilarity is presented instead in the same domain between the origin and the singularity for the solution. Starting from the left of the singularity to the origin, the solution to (24) (left solid black curve for small values of ξ) leaves the $(\xi - \xi_0)^{-1}$ curve (dotted black) determining its initial simple pole imprinting so to generate again a singularity at the origin, but this time progressing to the positive infinity value through a tan-type profile.

Having payed attention on consequences of initial conditions near the singularity, devised on the observation of dominant term (31) and solutions to (23), in order to having a more complete picture on the problem (24), it is worth to pursue the same strategy of screening the solutions that are isolated by the enforcement of data similar to that of an assigned reference function (26). However, at this time data are taken at some point far from singularities of Φ_0 . Stationary points can be chosen as reference for initial conditions, for instance. In figure 7, in particular, the solution to (24) is asked to develop the same local maxima of the function (26) with the off $\alpha_1 = -3$ and $\alpha_2 = 1$ (red dashed). A curve emerges that is not anymore anti-symmetric with respect to the vertical axis, and an asymptote comes after the maximum in a manner analogous to what we have formerly seen to progress from a superimposed vertical asymptote, see figure 6(b). To some extent, the Φ_0 -pattern is better preserved before the maximum, albeit it is evident that also the anti-symmetry between the maximum and the minimum breaks down. The latter is visibly lowered, like most of the curve in the $\xi < 0$ domain. The raising of the function to positive values in the proximity of the origin is also clear, and this contributes to the formation of a greater dip conducting to the minimum.

Graphs of figure 7 also illustrate what can be displayed by still taking $\Phi_0(\xi; -3, 1)$ as trial function to settle initial conditions for the ODE (24), but choosing points on it different from the maximum. In particular, we have considered points to the right of the maximum, where the function smoothly decays monotonically. With the diminishing of $\Phi_0(\xi; -3, 1)$ and $\Phi_0'(\xi; -3, 1)$ there is a general tendency to push down the maximum for Φ , which moves uniformly to the right, see magenta and brown curves in figures 7(a) and (b). A memory of the minimum developing for $\Phi_0(\xi; -3, 1)$ is also seen, but in the region $\xi < 0$ the function Φ

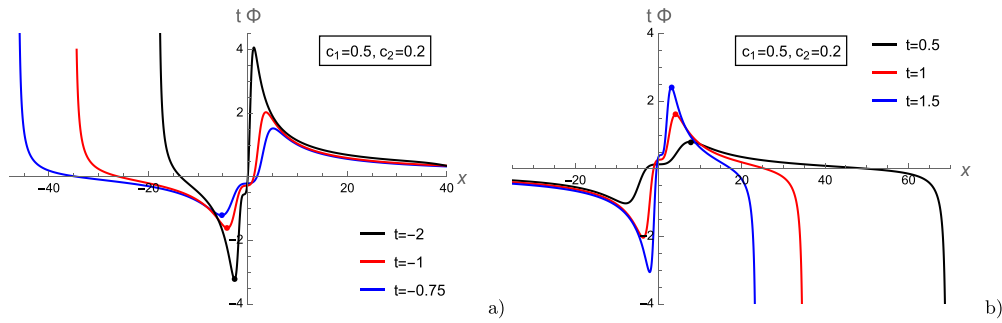


Figure 8. Examples of function $t\Phi(x, t)$ that consequent from (24) at different times and for $c_1 = 0.5, c_2 = 0.2$ and $\Delta = \eta^2 c_1^4$. Coloured dots refer to the initial value assignment for the function Φ coinciding with the maximum of (26) with $\alpha_1 = -3$ and $\alpha_2 = 1$. (a) Negative t . (b) Positive t .

does not experience the same flattening effect taking place for $\xi > 0$; see the magenta curve in figure 7(a). Actually, figure 7(b) shows that while the right part of the curve Φ attains lower values for smoother initial conditions (magenta and brown disks), the left part does not: the minimum for the magenta curve is actually less peaked than that of the brown curve which also tends to get back closer to origin. Also remark that the output profile for Φ can change abruptly in correspondence of certain initial conditions. This is shown by means of the blue curve in figure 7(a) whose shape evidently reminds the portion of Φ_0 developing on the right of the singularity for even negative α_1 and $\alpha_2 = 1$, but with in addition the newly introduced movable singularity standing out for positive ξ . This can be intuitively understood on the grounds that the choosing of initial conditions for Φ and Φ' may in practice act as selecting a Φ_0 with different pairs of α_1 and α_2 .

6.2. Remarks on solutions (21) to (1) for $\Delta \neq 0$

We have previously gained an insight on some peculiarities of a class of solutions to (22) and the next step would be arguing the pulling back to the original equation (1) acted via (21). The analysis of the effects on solutions to (1) can be prospected straight away founded on observations and guiding route put together for the case $\Delta = 0$ treated in section 4. We shall not argue therefore the complete casuistics for the choices that can be made for the coefficients c_j for it is very intelligible from (21). In figure 8, we therefore produce only the function $t\Phi$ determining solutions to (1) from the solution to (24) drawn in figure 7. The predicted flattening out during the evolution near $t = 0$, the exchange with reflections between the quadrants of the curve sections after the annulment at $t = 0$ and the amplification of the peaks in the later evolution are manifest. We conclude the section by emphasising that in potential applicative problems relying on equation (1) it may be also necessary to ascertain the consistency with possible constraint on domains of variables for the specific subject matter under study. For instance, if v is definite positive, those portions of the Φ curves have to be selected such that also the condition $v \geq 0$ comes true. Depending on the signs of structural coefficients c_j 's, in turn this demands taking into account either the condition $B\eta \frac{c_1^2}{c_3} t\Phi < 1$ or the condition $B\eta \frac{c_1^2}{c_3} t\Phi > 1$, where $B = 1$ if $\Delta = 0$ or $B = \Delta\eta^{-2}c_1^{-4}$ otherwise (equation (25)); i.e. either $\eta \frac{c_1^2}{c_3} t\Phi > 1$ or $\eta \frac{c_1^2}{c_3} t\Phi < 1$ for $\Delta = 0$, and either $\frac{\Delta}{\eta c_1^2 c_3} t\Phi > 1$ or $\frac{\Delta}{\eta c_1^2 c_3} t\Phi < 1$ if $\Delta \neq 0$.

7. N-pole dynamics of rational solutions

By looking at the equation (1) from the angle of local symmetry properties and similarity solutions, we have gained through the reduction (21) an interesting perspective on some pivotal characteristics owned by its solutions. The study we presented is clearly of limited extend, and the investigation of other fundamental features is in order. Among the open problems there is, for instance, the comprehension of aspects such as the existence of other distinctive classes of solutions and the possibility to proceed with their classification. In particular, shedding light on the existence of rational solutions comprising multiple simple poles seems to be a naturally due development. Indeed, singular solutions to remarkable integrable equations and their pole dynamics have proved to be intriguingly linked to the dynamics of particles in many-body systems (see, for instance, the seminal papers [36–38]) as well as to rogue waves (see [39–41]), and are still subject of active investigations about the rational solutions in the KP hierarchy and Painlevé equations [42–45]. In addressing this issue, guidelines can be taken from discussions concerning other integrable equations, as put forward for instance in [37]. The most natural connection in this respect clearly is seized with the standard Bateman–Burgers equation. In such a case, the existence of rational solutions and the analysis of their poles properties has been nicely investigated in [46], for instance. By proceeding similarly to [37, 46], the N -pole ansatz

$$v(x, t) = \eta\sigma \sum_{k=1}^N \frac{R_k(t)}{x - x_k(t)} \tag{34}$$

can be substituted in (1), and by later setting $x = x_j + \epsilon$, the resulting equation can be expanded in powers of ϵ . As in the Bateman–Burgers case, equating the most singular terms prompts to $R_k(t) = 1$. We observe here, however, that quite a more complex pole dynamics is suggested for rational solution of equation (1), at least when $\Delta \neq 0$. Indeed, by collecting terms at the successive order, one finds that the motion of poles $x_k(t)$ superimposed via (34) can be thus ascribed, at this level of approximation, to the concurrence of two mechanisms: a translation at fixed constant speed unavoidably entering in the matter once $c_1c_4 \neq 0$, and an additional motion obeying a nontrivial differential system. That is:

$$x_k(t) = -\frac{c_1c_4}{c_3^3}t + y_k(t) = \left(\frac{c_1}{c_2} - \frac{\Delta}{c_1c_3^2}\right)t + y_k(t), \tag{35}$$

where the functions $y_j(t)$ are determined by solutions of the following dynamical system:

$$\dot{y}_k(t) = \frac{\Delta}{c_3^3} \sum_{m=1}^{N-1} (m+1)! \left(-\frac{c_1}{c_3}\right)^{m-1} \eta^m \mathcal{P}_k^{(m)} \left[\{y_m\}_1^N\right], \quad \left(\cdot = \frac{d}{dt}\right), \tag{36}$$

the $\mathcal{P}_k^{(m)}$'s denoting the sum of products of distinct terms $(y_k - y_j)^{-1}$, i.e.

$$\mathcal{P}_k^{(1)} \left[\{y_m\}_1^N\right] = \sum_{\substack{j=1 \\ i \neq k}}^N \frac{1}{y_k - y_j}, \quad \mathcal{P}_k^{(2)} \left[\{y_m\}_1^N\right] = \sum_{\substack{j,m=1 \\ j,m \neq k \\ j \neq m}}^N \frac{1}{(y_k - y_j)(y_k - y_m)}, \tag{37}$$

$$\mathcal{P}_k^{(3)} \left[\{y_m\}_1^N\right] = \sum_{\substack{j,m,r=1 \\ j,m,r \neq k \\ j \neq m, j \neq r, m \neq r}}^N \frac{1}{(y_k - y_j)(y_k - y_m)(y_k - y_r)} \tag{38}$$

and so forth. The situation is therefore much different from the standard Bateman–Burgers equation with diffusivity η issuing for $c_1 \rightarrow 0$ (along with the normalisation conditions $c_3 = -c_2$ and $\sigma = -2$), for which the motion of poles entering a N -pole ansatz of the type (34) would be determined by the hamiltonian differential system $\dot{x}_k(t) = -2\eta\mathcal{P}_k^{(1)}[\{x_m\}_1^N]$. Then, there is an interaction among poles that is not limited to just pairwise couplings as it happens in the standard Bateman–Burgers equation [46]. The manner in which a pole $x_k(t)$ in (34) varies is ruled by its correlations with an increasing number of the other distinct poles, until all the poles appear. Two remarks are clearly in order on this statement. First, it has been assumed that $\Delta = c_1^2c_4 + c_2c_3^2 \neq 0$. When $\Delta = 0$ one is merely lead instead to t -linear translations of poles with rate $\dot{x}_k(t) = \frac{c_2}{c_1}t$. Secondly, under the circumstance that η is a small perturbation parameter, one may reason about disregarding higher-order terms in powers of η . By maintaining only the lowest order term in the right hand side of (36), the dynamical system governing the contribution $y_k(t)$ to the motion of poles $x_k(t)$ shares essentially the same form found in the Bateman–Burgers case:

$$\dot{y}_k(t) = 2\frac{\Delta}{c_3}\eta\mathcal{P}_k^{(1)}[\{y_m\}_1^N]. \tag{39}$$

The investigation of the differential system (36) goes beyond our current scopes. We limit ourselves to remark that complete integrability is expected to be evincible using the Cole–Hopf transformation and the relationship between equations (1) and (5).

8. Discussion and conclusions

In this communication, we have addressed the study of the nonlinear 1 + 1 dimensional PDE (1), i.e.

$$\partial_t v + \partial_x \left\{ \frac{1}{c_1 v + c_3 \sigma} [c_2 v^2 + c_4 \sigma^2 + \sigma \eta (c_1 \partial_t v + c_2 \partial_x v)] \right\} = 0,$$

representing a non-evolutive generalisation of known diffusive/dissipative equations. The equation has been introduced recently in [1] and ensues from rather general grounds. Indeed, it can be obtained from a 1+1 differential conservation law where: (i) the flux density depends both on the density and (linearly) from the first derivatives of density with respect to the local variables; (ii) the linearisability via a Cole–Hopf transform is demanded in addition. To date, very little is known on equation (1) and its solutions. When one or more of the coefficients c_j do vanish, some crucial simplifications may occur that enable to determine solutions almost effortlessly, as we commented in section 2.1. In particular, the simple tan-type (17) or rational solutions (18) are admitted. The circumstance definitively motivates the paying attention on the occurrence of singularities for solutions to (1).

In the present communication, by performing a similarity reduction dictated by one of the local symmetry generators underlying the equation (1), we have shown that a nonlinear ordinary differential equation arises which is connected to the PIII equation. While standard arguments concerning the existence of solutions with simple poles prove their usefulness, the discussion we presented here in this regard took quite a benefit from the circumstance that the model is exactly solvable in the special case where the constraint $\Delta = c_1^2c_4 + c_2c_3^2 = 0$ do hold. The general real solution thence originated takes a simple mathematical structure with a still rich dynamics and interesting key-elements, e.g. in respect to the presence of singularities how we have detailed. Regardless the potential marginal relevance of such a strict binding $\Delta = 0$ in concrete applications to specific problems, the circumstance of exact solvability provides indeed first remarkable hints concerning what to expect for solutions to the general differential

problem when $\Delta \neq 0$, at least within fairly identified assumptions and regimes. This allows for gaining a clue also on the unavoidable qualitative differences, such as the generation of additional divergences, as we argued in section 6 where the strategy of selecting solutions by tailoring them to an assigned solution pertaining $\Delta = 0$ has been pursued. We have been also attentive to the implications in respect to the t -dependent dynamics of poles and asymptotes for the solution, showing an inversion of their motions. These results put a basis for the understanding of the general case $\Delta \neq 0$, for which a more singular behaviour has been shown to emerge.

Future investigations concerned with (1) are definitively in order and they may naturally include both other mathematical issues and more applicative problems. We already understood in section 7 that a deeper comprehension of the integrability properties underlying the dynamics of multiple poles would be desirable, in a manner parallel to what has been done for the Bateman–Burgers equation for instance [46]. Another elucidation looks to be in respect to the identification of non-local symmetries. Besides providing insights on the possibility to have receipts for transferring possible analytical results, hints on the settling of diverse coordinate transformations may play a role as regards aspects like the reduction to normal form, classification of solutions and characterisation of possible correlated hierarchies in a way similar to the case of the non-evolutionary viscous scalar reduction of the two-component Camassa–Holm equation considered in [25]. Generalised symmetries determining Miura-type actions play indeed a decisive role in that framework. It would be also interesting to understand if they may enable to connect (1) to a Painlevé equation in the general case when $\Delta \neq 0$, as we have seen that for $\Delta = 0$ the equation is related to the PIII through a Cole–Hopf type transformation. Other developments may be more focused on the application of equation (1), including those for purposes potentially different from the fluid systems considered so far, such as in the context of complex systems based on mean-field spin models. The idea of formally describing the governing behaviour of relevant statistical quantities through the solutions of PDEs is starting to be appraised even for problems in reaction kinetics [47] and artificial intelligence [48], for instance. This may raise the question about the possible need to implement the model (3) while dealing with specific problems, such as by taking into account other non-local terms in the expansion that may cure or smoothen appearing criticalities and allow for the identification of multiple scales of both mathematical and applicative relevance. We finally mention that natural advances of the investigation performed in this work entail multi-component integrable conservation laws, for instance those arising in the treatment of nematic liquid crystal systems [23, 24]. Extension of our approach to integrable hydrodynamic chains may also prove to be insightful, e.g. in the context of random matrix models [49].

Data availability statement

All data that support the findings of this study are included within the article (and any supplementary files).

Acknowledgments

F G and G L would like to thank the *Isaac Newton Institute for Mathematical Sciences*, Cambridge, for support and hospitality during the programme *Dispersive hydrodynamics: mathematics, simulation and experiments, with applications in nonlinear waves* where work on this paper was undertaken. This work was supported by EPSRC grant no EP/R014604/1. F G also acknowledges the hospitality of the Lecce’s division of INFN and of the *Department of*

Mathematics and Physics ‘Ennio De Giorgi’ of the University of Salento. G L also acknowledges the hospitality of the School of Mathematics and Statistics of the University of Glasgow. G L and L M are partially supported by INFN IS-MMNLP. Authors are indebted with A Moro for useful discussions. G L thanks F Curto for suggestions leading to the improvement of the figures.

Appendix. Proofs of propositions 2–4

Proposition 2 (stationary points of solution (26) for integer values of α_1). *Let $\alpha_1 \in \mathbb{Z}$, $\alpha_2 > 0$, $\xi^{(0)} = 0$ and $\xi_{\pm}^c = \pm |\alpha_1(1 - \alpha_1)\alpha_2|^{\frac{1}{1-\alpha_1}}$. The stationary points of solution (26) are listed below.*

- (i) *Three stationary points located at $\xi = \xi^{(0)}$ (inflection point) and $\xi = \xi_{\pm}^c$ for α_1 odd negative integer with $\alpha_1 < -1$.*
- (ii) *Two stationary points when $\alpha_1 = -1$, located at $\xi = \xi_{\pm}^c$.*
- (iii) *Two stationary points for α_1 even negative integer, located at $\xi = \xi^{(0)}$ and $\xi = \xi_+^c$.*
- (iv) *One single stationary point located at $\xi = \xi_+^c$ for α_1 even positive integer.*
- (v) *Two stationary points for odd positive integers α_1 located at $\xi = \xi_{\pm}^c$.*

Proof. The proof is based on similar arguments used in proposition 1. The stationary points of (26) are given by the zeros of $\Phi'_0(\xi; \alpha_1, \alpha_2) = (\alpha_1 - 1) \frac{[\alpha_1(\alpha_1 - 1)\alpha_2\xi^{\alpha_1 - 1} - 1]}{[(\alpha_1 - 1)\alpha_2\xi^{\alpha_1} - \xi]^2}$.

Let us first consider the case $\alpha_1 \in \mathbb{Z}_{<0}$. The stationary points are given by the real roots of the polynomial $\tilde{\mathcal{P}}^-(\xi) := [\alpha_1(\alpha_1 - 1)\alpha_2 - \xi^{1-\alpha_1}] \xi^{\alpha_1 - 1}$. One root $\xi^{(0)} = 0$ arises for $\alpha_1 < -1$. One can verify that $\Phi''_0(\xi^{(0)}) = 0$, hence giving an inflection point. The other roots for negative integers are given by $\xi_l = |\alpha_1(1 - \alpha_1)\alpha_2|^{\frac{1}{1-\alpha_1}} e^{i\frac{2l\pi}{1-\alpha_1}}$, $l = 0, 1, \dots, -\alpha_1$. The real solution $\xi_+^c = |\alpha_1(1 - \alpha_1)\alpha_2|^{\frac{1}{1-\alpha_1}}$ is obtained when $l = 0$, while $\xi_-^c = -|\alpha_1(1 - \alpha_1)\alpha_2|^{\frac{1}{1-\alpha_1}}$ is obtained for α_1 odd when $l = \frac{1-\alpha_1}{2}$. These prove (i), (ii) and (iii).

Let us now consider the case $\alpha_1 \in \mathbb{Z}_{>0}$. The case $\alpha_1 = 1$ identifies the null solution as discussed earlier. When $\alpha_1 > 1$ we have that stationary points are real roots of the polynomial $\tilde{\mathcal{P}}^+(\xi) := \alpha_1(\alpha_1 - 1)\alpha_2\xi^{\alpha_1 - 1} - 1$, $\xi_l = |\alpha_1(1 - \alpha_1)\alpha_2|^{\frac{1}{1-\alpha_1}} e^{i\frac{2l\pi}{1-\alpha_1}}$, $l = 0, 1, \dots, \alpha_1 - 2$. We promptly identify the real root $\xi_+^c = |\alpha_1(1 - \alpha_1)\alpha_2|^{\frac{1}{1-\alpha_1}}$. A second real solution occurs for odd integers only, requiring $2l\pi = (1 - \alpha_1)\pi$, that is $l = \frac{1-\alpha_1}{2}$, giving $\xi_-^c = -|\alpha_1(1 - \alpha_1)\alpha_2|^{\frac{1}{1-\alpha_1}}$. These complete the proof of (iv) and (v). □

Proposition 3 (singularities of (26) for rational values of α_1). *Let $\alpha_1 = \frac{q}{p}$ with $q, p \in \mathbb{Z}$ and $\text{gcd}(q, p) = 1$, and consider $\xi^{(0)}$, ξ_{\pm} defined as in proposition 1. The real poles of (26) are listed below.*

- (i) *Case $\alpha_1 < 0$.*
 - (a) *One singularity located at $\xi = \xi_-$ (branch point) if p is odd and q is even.*
 - (b) *No singularities if p and q are odd.*
 - (c) *One singularity at $\xi = \xi_+$ (branch point) if p is even.*
- (ii) *Case $0 < \alpha_1 < 1$.*
 - (a) *Two singularities if p is odd and q is even located at $\xi = \xi^{(0)}$ (branch point) and $\xi = \xi_-$ (branch point).*

- (b) One singularity located at $\xi = \xi^{(0)}$ (branch point) if p and q are odd.
- (c) One singularity located at $\xi = \xi^{(0)}$ (branch point) if p is even.
- (iii) Case $\alpha_1 > 1$.
 - (a) Two singularities if p is odd and q is even located at $\xi = \xi^{(0)}$ (pole) and $\xi = \xi_+$ (branch point).
 - (b) Three singularities if p and q are odd located at $\xi = \xi^{(0)}$ (pole) and $\xi = \xi_{\pm}$ (branch points).
 - (c) Two singularities at $\xi = \xi^{(0)}$ (pole) and $\xi = \xi_+$ if p (branch point) is even.

Proof. Wlog, let $p \in \mathbb{Z}_{>0}$ and consider the above different cases as q varies in \mathbb{Z} . Note that for p even, the solution (26) is defined for $\xi \geq 0$. Also notice that the additional condition $\text{gcd}(q, p) = 1$ ensures that to each $\alpha_1 \in \mathbb{Q}$ we associate unambiguously a pair of integers (q, p) .

We will prove case (iii) as an example, $\alpha_1 > 1$. In this case, singularities are given by zeros of the polynomial $\mathcal{P}^+(\xi) := \xi [((\alpha_1 - 1)\alpha_2)\xi^{\frac{q-p}{p}} - 1]$. Clearly a singularity occurs at $\xi^{(0)} = 0$. Other real solutions are among the following $\xi_l = |\alpha_1(1 - \alpha_1)\alpha_2|^{\frac{1}{1-\alpha_1}} e^{ip\frac{2l\pi}{q-p}}$, $l = 0, 1, \dots, q - p - 1$. Real roots are obtained in two cases, either looking for l fulfilling $2pl = 2k(q - p)$ or $2pl = (2k + 1)(q - p)$ for some integer k . The former gives $\xi = \xi_+$, while the latter gives $\xi = \xi_-$. The parity of q and p implies the qualitative scenario. Indeed, $\xi = \xi_+$ arises for all parities of q and p , but the situation is different for $\xi = \xi_-$. Indeed, only when q and p are both odd (hence $q - p$ even), an additional solution is found at $\xi = \xi_-$. This proves (i).

Cases (i) and (ii) are derived following similar procedure and their proof is here omitted. In general, one has to identify the polynomial whose zero correspond to singularities of ϕ_0 , find the complex roots and select the real ones by looking at the parity of q and p . \square

Proposition 4 (stationary points of (26) for rational values of α_1). Let $\alpha_1 = \frac{q}{p}$ with $q, p \in \mathbb{Z}$ and $\text{gcd}(q, p) = 1$, and consider $\xi^{(0)}$, ξ_{\pm}^c defined as in proposition 2. The stationary points of (26) are listed below.

- (i) Case $\alpha_1 < 0$.
 - (a) Two stationary points located at $\xi = \xi^{(0)}$ and $\xi = \xi_+^c$ if p is odd and q is even.
 - (b) Three stationary points located at $\xi = \xi^{(0)}$ (inflection point) and $\xi = \xi_{\pm}^c$ if p and q are odd.
 - (c) Two stationary points located at $\xi = \xi^{(0)}$ and $\xi = \xi_+^c$ if p is even.
- (ii) Case $0 < \alpha_1 < 1$.
 - (a) One stationary point at $\xi = \xi_-^c$ if p is odd and q is even.
 - (b) No stationary points if p and q are odd.
 - (c) No stationary points if p is even¹³.
- (iii) Case $\alpha_1 > 1$.
 - (a) One stationary point located at $\xi = \xi_+^c$ if p is odd and q is even.
 - (b) Two stationary points located at $\xi = \xi_{\pm}^c$ if p and q are odd.
 - (c) One stationary point at $\xi = \xi_+^c$ if p is even.

Proof. Let $p \in \mathbb{Z}_{>0}$ and consider the above different cases as q varies in \mathbb{Z} . We will prove case (i) as an example, $\alpha_1 < 0$. In this case, stationary points are real zeros of the polynomial $P^-(\xi) = \xi^{-2\alpha_1} [\alpha_1(\alpha_1 - 1)\alpha_2 - \xi^{1-\alpha_1}]$. Clearly, $\xi = 0$ is always a stationary point. The other stationary points are the real roots among $\xi_l = |\alpha_1(\alpha_1 - 1)\alpha_2|^{\frac{1}{1-\alpha_1}} e^{i\frac{2\pi lp}{p-q}}$, $l = 0, 1, \dots, p - q -$

¹³ If one considers $\xi^p = -\sqrt[p]{\xi}$ a stationary point is located at $\xi = \xi_+^c$.

1. Real roots are obtained in two cases, either looking for l fulfilling $2pl = 2k(q - p)$ or $2pl = (2k + 1)(q - p)$ for some integer k . The former would imply $\xi = \xi_+^c$, while the latter would lead to $\xi = \xi_-^c$. A second stationary point located at $\xi = \xi_+^c$ arises for all parities of q and p . A third stationary point located at $\xi = \xi_-^c$ arises when p and q are odd only, hence proving (i). Cases (ii) and (iii) are derived following similar procedure and their proof is here omitted. \square

ORCID iDs

Francesco Giglio  <https://orcid.org/0000-0003-1131-1560>

Giulio Landolfi  <https://orcid.org/0000-0001-6699-7876>

Luigi Martina  <https://orcid.org/0000-0002-2858-7320>

References

- [1] Giglio F, Landolfi G and Moro A 2016 Integrable extended van der Waals model *Physica D* **333** 293–300
- [2] Bateman H 1915 Some recent research on the motion of fluids *Mon. Weather Rev.* **43** 163–70
- [3] Burgers J M 1939 *Mathematical Examples Illustrating Relations Occurring in the Theory of Turbulent Fluid Motion* (Verhandel. Kon. Nederl. Akad. Wetenschappen Amsterdam, Afd. Natuurkunde) pp 171–53
- [4] Burgers J M 1948 *A Mathematical Model Illustrating the Theory of Turbulence (Advances in Applied Mechanics vol 1)* ed R Von Mises and T Von Kármán (Academic) pp 171–99
- [5] Kolmogorov A, Petrovskii I and Piskunov N 1937 A study of the diffusion equation with increase in the amount of substance and its application to a biological problem *Bull. Moscow Univ., Math. Mech* **1** 1–25 transl. in Tikhomirov V M (ed) *Selected Works of A N Kolmogorov I*, 248–70, Kluwer, Dordrecht, 1991
- [6] Fokker A D 1914 Die mittlere energie rotierender elektrischer dipole im strahlungsfeld *Ann. Phys., Lpz.* **348** 810–20
- [7] Frank T D 2010 *Nonlinear Fokker-Planck Equations Fundamentals and Applications (Springer Series in Synergetics)* (Springer)
- [8] Murray J D 2013 *Mathematical Biology* (Springer)
- [9] Furioli G, Pulvirenti A, Terraneo E and Toscani G 2017 Fokker-Planck equations in the modeling of socio-economic phenomena *Math. Models Methods Appl. Sci.* **27** 115–58 and references therein
- [10] Calogero F 2017 New C-integrable and S-integrable systems of nonlinear partial differential equations *J. Nonlinear Math. Phys.* **24** 142–8
- [11] Krasilshchik I S and Vinogradov A M (eds) 1999 *Symmetries and Conservation Laws for Differential Equations of Mathematical Physics (Translation of Mathematical Monographs Series)* (AMS)
- [12] Olver P 1993 *Applications of Lie Groups to Differential Equations Graduate Texts in Mathematics vol 107* (Springer)
- [13] Svinolupov S I 1985 Analogs of the Burgers equation of arbitrary order *Theor. Math. Phys.* **65** 1177–80
- [14] Sokolov V V 1988 On the symmetries of evolution equations *Russ. Math. Surv.* **43** 165–204
- [15] Abramenko A A, Lagno V I and Samoilenko A M 2002 Group classification of nonlinear evolutionary equations: II. Invariance under solvable groups of local transformations *Differ. Equ.* **38** 502–9
- [16] Lagno V I and Samoilenko A M 2002 Group classification of nonlinear evolution equations. I. Invariance under semisimple local transformation groups *Differ. Equ.* **38** 384–91
- [17] Giglio F, Landolfi G, Martina L and Moro A 2021 Symmetries and criticality of generalised van der Waals models *J. Phys. A: Math. Theor.* **54** 405701
- [18] Barra A and Moro A 2015 Exact solution of the van der Waals model in the critical region *Ann. Phys., NY* **359** 290–9
- [19] Brankov J G and Zagrebnov V A 1983 On the description of the phase transition in the Husimi–Temperley model *J. Phys. A: Math. Gen.* **16** 2217–24

- [20] Brankov J G 1990 Derivation of finite-size scaling for mean-field models from the Burgers equation *J. Phys. A: Math. Gen.* **23** 5647–54
- [21] Choquard P and Wagner J 2004 On the mean field interpretation of Burgers equation *J. Stat. Phys.* **116** 843–53
- [22] Barra A, Del Ferraro G and Tantari D 2013 Mean field spin glasses treated with PDE techniques *Eur. Phys. J. B* **86** 332
- [23] De Matteis G, Giglio F and Moro A 2018 Exact equations of state for nematics *Ann. Phys., NY* **396** 386–96
- [24] De Matteis G, Giglio F and Moro A 2023 Complete integrability and equilibrium thermodynamics of biaxial nematic systems with discrete orientational degrees of freedom (arXiv:2309.13293)
- [25] Arsie A, Lorenzoni P and Moro A 2015 Integrable viscous conservation laws *Nonlinearity* **28** 1859–95
- [26] Kevorkian J 1990 *Partial Differential Equations: Analytical Solution Techniques* (Brooks/Cole Pub. Company)
- [27] Abd-el-Maleka M B and El-Mansib S M A 2000 Group theoretic methods applied to Burgers' equation *J. Comp. Appl. Math.* **115** 1–12
- [28] Moro A 2014 Shock dynamics of phase diagrams *Ann. Phys., NY* **343** 49–60
- [29] Whitham G B 1974 *Linear and Nonlinear Waves* (Wiley)
- [30] Conte R and Musette M 2020 *The Painlevé Handbook* (Springer Nature)
- [31] Clarkson P A 2003 Painlevé equations-nonlinear special functions *J. Comput. App. Math.* **153** 127–40
- [32] Ferapontov E V, Huard B and Zhang A 2012 On the central quadric ansatz: integrable models and Painlevé reductions *J. Phys. A: Math. Theor.* **45** 195204
- [33] Morse P M and Feshbach H 1953 *Methods of Theoretical Physics, Part I* (McGraw-Hill)
- [34] Conte R (ed) 1999 *The Painlevé Property: One Century Later (CRM Series in Mathematical Physics)* (Springer)
- [35] Hone A N W 2009 Painlevé tests, singularity structure and integrability *Integrability (Lecture Notes in Physics vol 767)* ed A V Mikhailov (Springer) ch 7, pp 245–77
- [36] Airault H, McKean H P and Moser J 1977 Rational and elliptic solutions of the Korteweg-de Vries equation and a related many-body problem *Commun. Pure Appl. Math.* **30** 95–148
- [37] Choodnovsky D V and Choodnovsky G V 1977 Pole expansions of nonlinear partial differential equations *Nuovo Cim.* **B40** 339–53
- [38] Calogero F, Olshanetsky M A and Perelomov A M 1979 Rational solutions of the KdV equation with damping *Lett. Nuovo Cim.* **24** 97–100
- [39] Dubard P and Matveev V B 2013 Multi-rogue wave solutions: from the NLS to the KP-I equation *Nonlinearity* **26** 93–125
- [40] Gaillard P 2011 Families of quasi-rational solutions of the NLS equation and multi-rogue waves *J. Phys. A: Math. Theor.* **44** 1–15
- [41] Clarkson P A and Dowie E 2017 Rational solutions of the Boussinesq equation and applications to rogue waves *Trans. Math. Appl.* **1** 2398–4945
- [42] Clarkson P A and Dunning C 2023 Rational solutions of the fifth Painlevé equation. Generalised Laguerre polynomials (arXiv:2304.01579)
- [43] Zabrodin A 2019 Elliptic solutions to integrable nonlinear equations and many-body systems *J. Geom. Phys.* **146** 103506
- [44] Rudneva D and Zabrodin A 2020 Dynamics of poles of elliptic solutions to the BKP equation *J. Phys. A: Math. Theor.* **53** 075202
- [45] Prokofev V V and Zabrodin A V 2021 Elliptic solutions of the Toda lattice hierarchy and the elliptic Ruijsenaars-Schneider model *Theor. Math. Phys.* **208** 1093–115
- [46] Deconinck B, Yo K and Segur H 2007 The pole dynamics of rational solutions of the viscous Burgers equation *J. Phys. A: Math. Theor.* **40** 54–59
- [47] Agliari E, Barra A, Landolfi G, Murciano S and Perrone S 2018 Complex reaction kinetics in chemistry: a unified picture suggested by mechanics in physics *Complexity* **2018** 7423297
- [48] Agliari E, Fachechi A and Marullo C 2022 Nonlinear PDEs approach to statistical mechanics of dense associative memories *J. Math. Phys.* **63** 103304
- [49] Benassi C, Dell'Atti M and Moro A 2021 Symmetric matrix ensemble and integrable hydrodynamic chains *Lett. Math. Phys.* **111** 78